Proceedings of International Physics Conference (2025) 1 (1): 27-35
https://proceedings.fisikaupi.id/index.php/ipc
ISSN 2986-9544 (Online)

DFT-Based Electronic and Xanes Spectra of Pd@Au$_{12}$ and Au$_{13}$ Nanoclusters for Antibiotic Sensing Applications

Hilman Fauzan, Lilik Hasanah, Endi Suhendi

This article has been presented at The 2nd International Physics Conference (IPC)
Universitas Pendidikan Indonesia, Bandung, Indonesia.
August, 16, 2025

Abstract

The development of effective and efficient sensors is crucial in facing the challenge of antibiotic resistance. Gold and palladium nanoclusters show enormous potential in antibiotic sensor applications. This study aimed to analyze the electronic properties, specifically the Density of States (DOS) and Partial Density of States (PDOS), and the optical properties, such as X-ray Absorption Near Edge Structure (XANES), of Pd@Au12 and Au13 as materials for antibiotic sensors. Calculations were performed using Density Functional Theory (DFT) with the GGA-PBE functional approach and the PAW scalar relativistic method for the interaction between valence electrons and the atomic core. The optimization results of the Pd@Au12 and Au13 structures maintained a stable icosahedral structure with a size of 0.468 nm. The Density of States analysis consistently showed metallic characteristics for both Pd@Au12 and Au13, with the Fermi energy of Pd@Au12 at -4.738 eV, slightly higher than that of Au13 at -5.2663 eV, indicating increased reactivity. The Partial Density of States revealed the hybridization of the Pd 4d orbital with the Au 5d orbital. The Pd K-edge XANES spectra indicated the availability of unoccupied 4p orbitals in the Pd atom, confirming its central role in reactivity. All these properties indicated a strong potential for these materials as sensors. This study laid a solid foundation for understanding nanocluster interactions in the future development of antibiotic sensors.

Keywords: *Antibiotic Resistance · Antibiotic Sensors · Gold-Palladium Nanoclusters · Density Functional Theory · XANES*

INTRODUCTION

Antibiotic resistance represent one of the most pressing global health threats of the 21st century, challenging the efficacy of treatments for bacterial infections and leading to increased morbidity and mortality (Chinemerem Nwobodo et al., 2022). This crisis, exacerbated by the misuse and overuse of antibiotics, necessitates the development of innovative strategies for the early detection and monitoring of resistant pathogens (Elbehiry et al., 2025). Consequently, the creation of effective and efficient sensors is crucial for mitigating this threat. Such sensors, capable of the rapid and accurate detection of antibiotics or resistant bacteria, can facilitate improved diagnostics and curb the spread of resistant strains (Guliy et al., 2022).

In the pursuit of advanced sensors, nanoscale materials, particularly metallic nanoclusters, have garnered significant attention owing to their unique electronic and optical properties, which hold immense promise for biosensing applications. Gold (Au) and Palladium (Pd)

✉ Hilman Fauzan
hilmanfauzan29@upi.edu
Endi Suhendi
endis@upi.edu
Lilik Hasanah
lilikhasanah@upi.edu

Physics Study Program, Universitas Pendidikan Indonesia, Bandung, Indonesia

How to Cite: Fauzan, H., Hasanah, L., & Suhendi, E. (2025). DFT-Based Electronic and Xanes Spectra of Pd@Au12 and Au13 Nanoclusters for Antibiotic Sensing Applications. *Proceedings of International Physics Conference, 1*(1), 27-35. https://proceedings.fisikaupi.id/index.php/ipc

nanoclusters, in particular, have emerged as excellent candidates for the core sensing material (Du et al., 2020; Kumar et al., 2017). Their distinct characteristics stemming from quantum size effect, such as a high surface area to volume ratio and enhanced reactivity, make them ideal platforms for antibiotic detection (Draviana et al., 2023; Nasrollahpour et al., 2023a). However, an atomic-level understanding of bimetallic nanoclusters such as Au13 and Pd@Au12 remains limited. This knowledge gap impedes the rational design and optimization of nanocluster-based sensors. (Chu et al., 2025).

This study aims to bridge this gap by conducting a comprehensive analysis of the electronic properties, specifically the Density of State (DOS) and Partial Density of State (PDOS) and optical properties, characterized by the X-ray Absorption Near Edge Structure (XANES) of Au13 and Pd@Au12 nanoclusters. Our analysis employs Density Functional Theory (DFT) calculations, utilizing the GGA-PBE functional for the exchange correlation energy and the scalar relativistic Projector Augmented Wave (PAW) method. A fundamental understanding of these properties is crucial for predicting and elucidating the nanoclusters behavior upon interaction with antibiotic analytes. Ultimately, these findings are expected to provide a robust theoretical foundation to guide the future development of more sophisticated and efficient antibiotic sensors, thereby contributing to the global effort against the antibiotic resistance crisis.

METHOD

This study employed a theoretical computational approach based on first-principles quantum mechanics. This ab initio methodology was selected to facilitate an in-depth, atomic-scale analysis of the nanoclusters electronic and optical properties without the need for physical laboratory experiments (Tran & Guidez, 2020). All simulations were executed using the Quantum Espresso software package, with calculations performed on the Mahameru BRIN high-performance computing (HPC) system.

The investigation focused on the bimetallic $Pd@Au_{12}$ core-shell and monometallic Au_{13} nanoclusters, chosen for their promising potential as advanced sensor materials for antibiotic detection. The computational procedure began with the geometry optimization of both nanoclusters to identify their most stable, lowest-energy configurations, maintaining an icosahedral structure found to be stable at a size of 0.468 nm. All calculations were conducted within the Density Functional Theory (DFT) framework (Zhu et al., 2022). The Perdew-Burke-Ernzerhof (PBE) parameterization of the Generalized Gradient Approximation (GGA) was utilized for the exchange-correlation functional (Khan et al., 2024). The electron-core interactions were described using the scalar-relativistic Projector Augmented Wave (PAW) method (Ciuk et al., 2024). Following optimization, we calculated the electronic properties, including the Density of States (DOS) to ascertain the metallic character and the Partial Density of States (PDOS) to delineate the specific contributions of Pd 4d and Au 5d orbitals and investigate orbital hybridization (da Silva et al., 2024). Finally, the optical properties were analyzed by computing the X-ray Absorption Near Edge Structure (XANES) at the Pd K-edge to probe the unoccupied 4p states, a key indicator of chemical reactivity (Huang et al., 2021; Iglesias-Juez et al., 2022; Orduz et al., 2024).

Post-processing and analysis of the simulation data were performed using specialized visualization software (Mortensen et al., 2024). The DOS and PDOS curves were analyzed to

identify the metallic nature, locate the Fermi level, and quantify the hybridization between Pd and Au orbitals (Kushwaha & Goel, 2025; Wang & Zhou, 2022). The Pd K-edge XANES spectra were interpreted to confirm the availability of unoccupied orbitals, which directly correlates to the reactivity of the Pd atom (Westawker et al., 2023a). These collective findings were then comprehensively interpreted to evaluate the potential of these nanoclusters as antibiotic sensors, emphasizing how their intrinsic electronic and optical properties could enhance sensory performance.

RESULTS AND DISCUSSION

Results

The geometries of the Au_{13} and $Pd@Au_{12}$ nanoclusters with a size 0.468 nm were optimized using Density Functional Theory (DFT). Following optimization, both nanoclusters retained a stable icosahedral structure, as depicted in Figure 1. The $Pd@Au_{12}$ nanoclusters exhibits a core-shell architecture, with a central palladium (Pd) atom encapsulated by a shell of 12 gold atoms. For the optimized $Pd@Au_{12}$ structure, the average Pd-Au bond distance was determined to be 0.2751 nm, while the average interatomic Au-Au distance within the shell was 0.3943 nm.

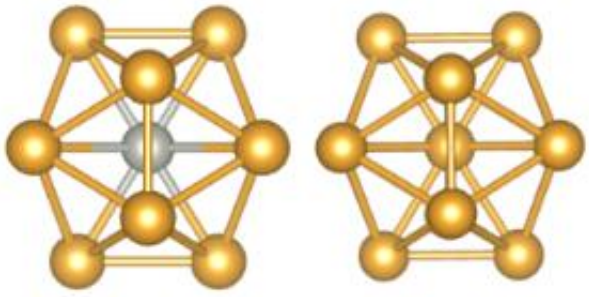

Figure 1. Optimized geometric structures of (left) the $Pd@Au_{12}$ core-shell and (right) the Au_{13} nanocluster

The total Density of States (DOS) for the $Pd@Au_{12}$ and Au_{13} nanoclusters is presented in Figures 2A and 2B, respectively.

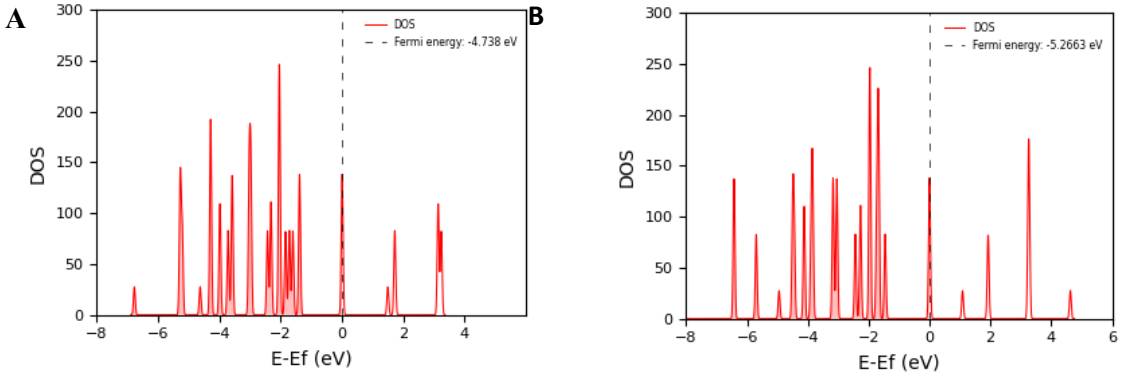

Figure 2. The total Density of States (DOS) for (A) the $Pd@Au_{12}$ nanocluster and (B) the Au_{13} nanocluster

The calculated energies of the Highest Occupied Molecular Orbital (HOMO), Lowest Unoccupied Molecular Orbital (LUMO), and the Fermi level for the $Pd@Au_{12}$ and Au_{13} nanoclusters are summarized in Table 1.

Table 1. Calculated HOMO, LUMO, and Fermi energies for the $Pd@Au_{12}$ and Au_{13} nanoclusters

No.	Parameter	Nanocluster	Value (eV)	Description
1.	E_{HOMO}	$Pd@Au_{12}$	-4.7311	Highest Occupied Molecular Orbital
2.	E_{LUMO}	$Pd@Au_{12}$	-3.2404	Lowest Unoccupied Molecular Orbital
3.	E_F (Fermi Energy)	$Pd@Au_{12}$	-4.738	Fermi Energy (0 eV reference in DOS plot)
4.	E_{HOMO}	Au_{13}	-4.8907	Highest Occupied Molecular Orbital
5.	E_{LUMO}	Au_{13}	-3.8418	Lowest Unoccupied Molecular Orbital
6.	E_F (Fermi Energy)	Au_{13}	-5.2663	Fermi Energy (0 eV reference in DOS plot)

To elucidate the individual orbital contributions to the electronic structure, a Partial Density of States (PDOS) analysis was performed. The resulting PDOS for the $Pd@Au_{12}$ and Au_{13} nanoclusters are depicted in Figures 3A and 3B, respectively.

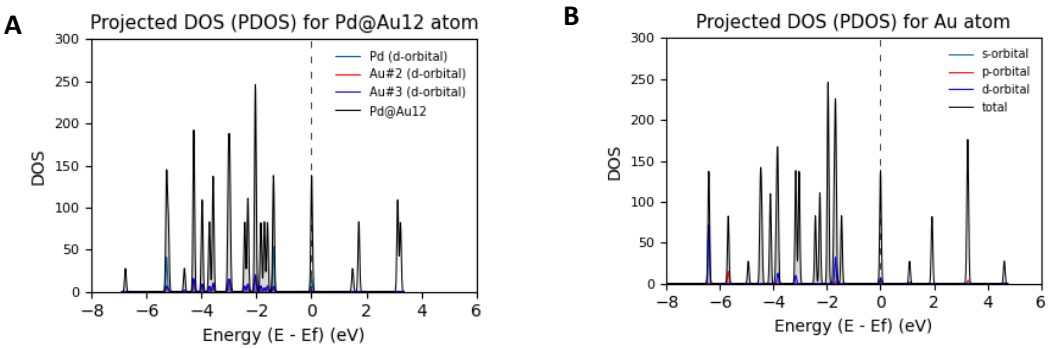

Figure 3. The Partial Density of States (PDOS) calculated for (A) the $Pd@Au_{12}$ core-shell and (B) the Au_{13} nanocluster

The calculated XANES spectrum of the $Pd@Au_{12}$ nanocluster, depicted in Figure 4, is characterized by an intense, sharp absorption peak at the absorption edge, commonly referred to as a "white line." Following this prominent feature, the spectrum exhibits a series of well-defined post-edge oscillations at higher energies.

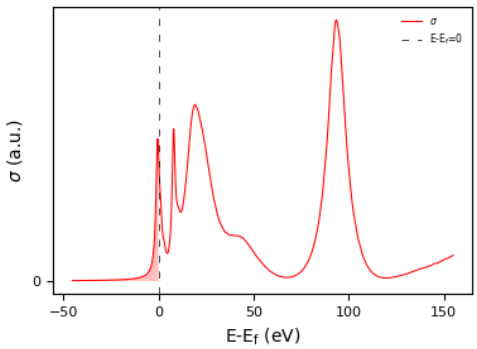

Figure 4. The calculated Pd K-edge XANES spectrum for the $Pd@Au_{12}$ nanocluster

Discussion

The simulated Au_{13} and $Pd@Au_{12}$ nanoclusters both exhibited a stable icosahedral geometry, which is consistent with previous findings that identify this as the most energetically

favorable conformation for small d-metal nanoparticles (Wang et al., 2025). In the $Pd@Au_{12}$ core-shell structure, the average Pd-Au bond length of 0.2751 nm indicates a strong interaction between the palladium core and the gold shell. This inherent structural stability provides a reliable foundation for the subsequent analysis of their electronic properties.

The Density of States (DOS) analysis in Figures 2A and 2B confirms the metallic character of both the Au_{13} and $Pd@Au_{12}$ nanoclusters. This is evidenced by the continuous, non-zero density of states at the Fermi level, a hallmark of metallic systems that facilitates electron mobility. Notably, the Fermi level of the $Pd@Au_{12}$ nanocluster is upshifted relative to that of the pure Au_{13} nanocluster. This upward energy shift suggests a higher population of available electronic states at the Fermi level, a feature generally correlated with enhanced chemical reactivity. The sharp, distinct peaks observed in the DOS plots are indicative of discrete energy levels, a hallmark of quantum confinement effects in nanoscale materials.

For the $Pd@Au_{12}$ nanocluster, the calculations in Table 1 reveal that the Highest Occupied Molecular Orbital (HOMO) is nearly degenerate with the Fermi level, while the Lowest Unoccupied Molecular Orbital (LUMO) is also energetically proximate. The sharp, distinct peaks observed in the DOS plots in Figures 2A and 2B are indicative of discrete energy levels, a hallmark of quantum confinement effects in nanoscale materials. The existence of substantial states both below and above the Fermi level further corroborates the metallic nature of these nanoclusters. The density of unoccupied states immediately above the Fermi level corresponds to the calculated LUMO, signifying the availability of low-lying empty orbitals that can act as electron acceptors.

The subtle differences in the DOS near the Fermi level between Au_{13} and $Pd@Au_{12}$ are attributed to the hybridization of Pd 4d and Au 5d orbitals, a conclusion supported by the PDOS analysis shown in Figures 3A and 3B. Figure 3A reveals that the total DOS of $Pd@Au_{12}$ is predominantly governed by the d-orbitals of both Pd and Au atoms, which exhibit significant hybridization across a wide energy range, particularly near the Fermi level. Conversely, the PDOS of pure Au_{13} is almost exclusively dominated by Au 5d orbitals, with only negligible contributions from the 6s and 6p orbitals, reflecting its elemental character. The pronounced contribution from the Pd 4d orbitals near the Fermi level in the bimetallic cluster underscores the pivotal role of the palladium dopant in governing the nanocluster's reactivity compared to its monometallic counterpart. This hybridization creates a high density of accessible electronic states at the Fermi level, priming the $Pd@Au_{12}$ nanocluster for interaction with external molecules.

The Pd K-edge XANES spectrum for the $Pd@Au_{12}$ nanocluster, depicted in Figure 4, offers crucial insights into the local electronic and structural environment of the central palladium atom (Marcella et al., 2020). The prominent, sharp peak at the absorption edge, known as the "white line," arises from the electronic transition of a 1s core electron to unoccupied states of p-symmetry (primarily 4p orbitals) above the Fermi level (Henderson et al., 2014). Notably, our theoretically calculated absorption edge energy is in good agreement with the reported experimental value of 24350 eV (Westawker et al., 2023b). The intensity and position of this white line are directly correlated with the density of unoccupied 4p states and the effective valence of the Pd atom. This finding corroborates the DOS and PDOS analyses, which also indicated enhanced reactivity stemming from the electronic states near the Fermi level.

Moreover, the extended energy range of the spectrum reveals detailed post-edge features, including the characteristic oscillations of the Extended X-ray Absorption Fine Structure (EXAFS) region. These oscillations arise from the backscattering of the emitted photoelectron by neighboring Au atoms in the icosahedral shell, thereby indirectly validating the local coordination environment of the central Pd atom (Sharma et al., 2023). Collectively, the Pd K-edge spectrum indicates that the central Pd atom possesses unoccupied 4p states ready to accept electrons, which is a finding consistent with the nanocluster's

metallic character and predicted reactivity, thereby affirming its role as a primary site for interaction with target molecules.

While XANES is an X-ray technique that does not directly probe optical properties in the visible range, the insights it provides into unoccupied electronic states and charge transfer are highly relevant for predicting changes in optical behavior (Abrosimov et al., 2024). Any alterations to the white line and other XANES feature upon interaction with an antibiotic molecule would signify modifications to the electronic distribution around the Pd atom. These electronic modifications can, in turn, alter how the nanocluster interacts with visible or ultraviolet photons, potentially leading to detectable shifts in its absorption, reflectance, or fluorescence spectra. Such optical changes could then be exploited as the transduction principle for an optical sensor. Thus, the XANES data not only confirms the nanocluster's intrinsic electronic reactivity but also provides a fundamental rationale for its potential optical response in sensing applications. Specifically, variations in the white line and post-edge features after analyte interaction would serve as key indicators of charge transfer or valence state changes in the Pd atom, thereby elucidating the underlying sensing mechanism.

For both $Pd@Au_{12}$ and Au_{13}, while the DOS plots exhibit discrete peaks with apparent gaps between them due to quantum confinement, it is crucial to clarify that these nanoclusters do not possess a true band gap in the semiconductor sense. Instead, their Fermi level falls within a continuum of accessible electronic states. This non-zero density of states at the Fermi level ensures high electronic conductivity, which is the defining characteristic of their metallic nature at the nanoscale.

The inherent metallic nature of both nanoclusters, characterized by a high density of states at the Fermi level, is a crucial attribute for their potential in sensing applications (Nasrollahpour et al., 2023b). This abundance of readily accessible electrons suggests a high reactivity towards target molecules such as antibiotics. Specifically, the upward shift of the Fermi level in $Pd@Au_{12}$, combined with the Pd-Au d-orbital hybridization, demonstrates that palladium doping effectively tunes the surface electronic properties. This conclusion is further corroborated by the Pd K-edge XANES data, which confirms the presence of unoccupied orbitals on the Pd atom poised to optimize analyte interactions. This contrasts sharply with semiconductor materials, which possess a distinct band gap between their valence and conduction bands (Antoine et al., 2023). Such a band gap would impede electron mobility and necessitate a higher activation energy for interactions, potentially compromising sensor sensitivity and response time. Consequently, the metallic character of these nanoclusters, particularly the fine-tuned electronic structure of $Pd@Au_{12}$ is expected to translate into superior sensor performance, offering both enhanced sensitivity and faster response rates.

CONCLUSION

In conclusion, this comprehensive Density Functional Theory study suggests that $Pd@Au_{12}$ and Au_{13} nanoclusters have strong potential due to their electronic and optical properties for antibiotic sensing applications. Both systems maintain a stable icosahedral geometry, which underpins their intrinsic characteristics. The DOS analysis confirms a crucial metallic character for both nanoclusters, with $Pd@Au_{12}$ exhibiting an upshifted Fermi level that indicates enhanced reactivity. This heightened reactivity is attributed to significant hybridization between the Pd 4d and Au 5d orbitals, which creates rich electronic pathways for molecular interaction. Furthermore, Pd K-edge XANES analysis points to the presence of available unoccupied 4p orbitals, affirming the central role of the palladium dopant in the material's reactivity and

marking it as a primary interaction site. Collectively, these results show that the unique properties of the Pd@Au_{12} nanocluster, engineered through palladium doping, fundamentally enhance its sensing potential. This work provides a robust theoretical foundation for bimetallic nanoclusters and recommends future studies involving direct simulations with antibiotic molecules to validate the predicted performance and elucidate the detailed sensing mechanisms.

ACKNOWLEDGMENT

The author gratefully acknowledges the computational resources provided by the National Research and Innovation Agency of Indonesia (BRIN). The computation in this work has been done using the facilities of MAHAMERU BRIN HPC, National Research and Innovation Agency of Indonesia (BRIN).

REFERENCES

Abrosimov, S., Protsenko, B., Mannaa, A., Vlasenko, V., Guda, S., Pankin, I., Burlov, A., Koshchienko, Y., Guda, A., & Soldatov, A. (2024). Improving sensitivity of XANES structural fit to the bridged metal-metal coordination. 447–455. https://doi.org/https://doi.org/10.1107/s1600577524002091

Antoine, R., Broyer, M., & Dugourd, P. (2023). Metal nanoclusters: from fundamental aspects to electronic properties and optical applications. In Science and Technology of Advanced Materials (Vol. 24, Issue 1). Taylor and Francis Ltd. https://doi.org/10.1080/14686996.2023.2222546

Chinemerem Nwobodo, D., Ugwu, M. C., Oliseloke Anie, C., Al-Ouqaili, M. T. S., Chinedu Ikem, J., Victor Chigozie, U., & Saki, M. (2022). Antibiotic resistance: The challenges and some emerging strategies for tackling a global menace. In Journal of Clinical Laboratory Analysis (Vol. 36, Issue 9). John Wiley and Sons Inc. https://doi.org/10.1002/jcla.24655

Chu, H. W., Demissie, G. G., Huang, C. C., & Anand, A. (2025). Protein-templated metal nanoclusters for chemical sensing. In Frontiers in Analytical Science (Vol. 5). Frontiers Media SA. https://doi.org/10.3389/frans.2025.1510588

Ciuk, T., Pyrzanowska, B., Jagiełło, J., Dobrowolski, A., Czołak, D., & Szary, M. J. (2024). Quasi-free-standing epitaxial graphene on 4H-SiC(0001) as a two-dimensional reference standard for Kelvin Probe Force Microscopy. Applied Surface Science, 675. https://doi.org/10.1016/j.apsusc.2024.160958

da Silva, K. N., Shetty, S., Sullivan−Allsop, S., Cai, R., Wang, S., Quiroz, J., Chundak, M., dos Santos, H. L. S., Abdelsalam, I. M., Oropeza, F. E., de la Peña O'Shea, V. A., Heikkinen, N., Sitta, E., Alves, T. V., Ritala, M., Huo, W., Slater, T. J. A., Haigh, S. J., & Camargo, P. H. C. (2024). Au@AuPd Core-Alloyed Shell Nanoparticles for Enhanced Electrocatalytic Activity and Selectivity under Visible Light Excitation. ACS Nano, 18(35), 24391–24403. https://doi.org/10.1021/acsnano.4c07076

Draviana, H. T., Fitriannisa, I., Khafid, M., Krisnawati, D. I., Widodo, Lai, C. H., Fan, Y. J., & Kuo, T. R. (2023). Size and charge effects of metal nanoclusters on antibacterial mechanisms. In Journal of Nanobiotechnology (Vol. 21, Issue 1). BioMed Central Ltd. https://doi.org/10.1186/s12951-023-02208-3

Du, X., Dong, W., Li, Z., Wen, G., Liu, M., & Fan, X. (2020). A novel nanosensor for detecting tetracycline based on fluorescent palladium nanoclusters. New Journal of Chemistry, 44(22), 9248–9254. https://doi.org/10.1039/c9nj06218a

Elbehiry, A., Marzouk, E., Abalkhail, A., Abdelsalam, M. H., Mostafa, M. E. A., Alasiri, M., Ibrahem, M., Ellethy, A. T., Almuzaini, A., Aljarallah, S. N., Abu-Okail, A., Marzook, N., Alhadyan, S., & Edrees, H. M. (2025). Detection of antimicrobial resistance via state-of-the-art technologies versus conventional methods. In Frontiers in Microbiology (Vol. 16). Frontiers Media SA. https://doi.org/10.3389/fmicb.2025.1549044

Guliy, O. I., Zaitsev, B. D., Smirnov, A. V., Karavaeva, O. A., & Borodina, I. A. (2022). Prospects of acoustic sensor systems for antibiotic detection. Biosensors and Bioelectronics: X, 12. https://doi.org/10.1016/j.biosx.2022.100274

Henderson, G. S., de Groot, F. M. F., & Moulton, B. J. A. (2014). X-ray absorption near-edge structure (XANES) spectroscopy. In Spectroscopic Methods in Mineralogy and Materials Sciences (pp. 75–138). De Gruyter. https://doi.org/10.2138/rmg.2014.78.3

Huang, J., Deng, F., Gunther, B., Achterhold, K., Liu, Y., Jentys, A., Lercher, J. A., Dierolf, M., & Pfeiffer, F. (2021). Laboratory-scale: In situ X-ray absorption spectroscopy of a palladium catalyst on a compact inverse-Compton scattering X-ray beamline. Journal of Analytical Atomic Spectrometry, 36(12), 2649–2659. https://doi.org/10.1039/d1ja00274k

Iglesias-Juez, A., Chiarello, G. L., Patience, G. S., & Guerrero-Pérez, M. O. (2022). Experimental methods in chemical engineering: X-ray absorption spectroscopy—XAS, XANES, EXAFS. In Canadian Journal of Chemical Engineering (Vol. 100, Issue 1, pp. 3–22). John Wiley and Sons Inc. https://doi.org/10.1002/cjce.24291

Khan, U., Saeed, M. U., Elansary, H. O., Moussa, I. M., Bacha, A. U. R., & Saeed, Y. (2024). A DFT study of bandgap tuning in chloro-fluoro silicene. RSC Advances, 14(7), 4844–4852. https://doi.org/10.1039/d3ra07452h

Kumar, N., Rosy, & Goyal, R. N. (2017). Gold-palladium nanoparticles aided electrochemically reduced graphene oxide sensor for the simultaneous estimation of lomefloxacin and amoxicillin. Sensors and Actuators, B: Chemical, 243, 658–668. https://doi.org/10.1016/j.snb.2016.12.025

Kushwaha, A., & Goel, N. (2025). First-principles investigation of Pd nanoclusters on MoTe2 for sensing SF6 decomposition gases. Surfaces and Interfaces, 59, 105939. https://doi.org/https://doi.org/10.1016/j.surfin.2025.105939

Marcella, N., Liu, Y., Timoshenko, J., Guan, E., Luneau, M., Shirman, T., Plonka, A. M., Van Der Hoeven, J. E. S., Aizenberg, J., Friend, C. M., & Frenkel, A. I. (2020). Neural network assisted analysis of bimetallic nanocatalysts using X-ray absorption near edge structure spectroscopy. Physical Chemistry Chemical Physics, 22(34), 18902–18910. https://doi.org/10.1039/d0cp02098b

Mortensen, J. J., Larsen, A. H., Kuisma, M., Ivanov, A. V., Taghizadeh, A., Peterson, A., Haldar, A., Dohn, A. O., Schäfer, C., Jónsson, E. Ö., Hermes, E. D., Nilsson, F. A., Kastlunger, G., Levi, G., Jónsson, H., Häkkinen, H., Fojt, J., Kangsabanik, J., Sødequist, J., … Thygesen, K. S. (2024). GPAW: An open Python package for electronic structure calculations. Journal of Chemical Physics, 160(9). https://doi.org/10.1063/5.0182685

Nasrollahpour, H., Sánchez, B. J., Sillanpää, M., & Moradi, R. (2023a). Metal Nanoclusters in Point-of-Care Sensing and Biosensing Applications. In ACS Applied Nano Materials (Vol. 6, Issue 14, pp. 12609–12672). American Chemical Society. https://doi.org/10.1021/acsanm.3c01569

Nasrollahpour, H., Sánchez, B. J., Sillanpää, M., & Moradi, R. (2023b). Metal Nanoclusters in Point-of-Care Sensing and Biosensing Applications. In ACS Applied Nano Materials (Vol. 6, Issue 14, pp. 12609–12672). American Chemical Society. https://doi.org/10.1021/acsanm.3c01569

Orduz, H. A. S., Bugarin, L., Heck, S. L., Dolcet, P., Casapu, M., Grunwaldt, J. D., & Glatzel, P. (2024). L3-edge X-ray spectroscopy of rhodium and palladium compounds. Journal of Synchrotron Radiation, 31(Pt 4), 733–740. https://doi.org/10.1107/S1600577524004673

Sharma, S. K., Johannessen, B., Golovko, V. B., & Marshall, A. T. (2023). X-ray Absorption Spectroscopy of Phosphine-Capped Au Clusters. Inorganics, 11(5). https://doi.org/10.3390/inorganics11050191

Tran, A. L., & Guidez, E. B. (2020). Quantum Mechanical Modeling of the Interactions between Noble Metal (Ag and Au) Nanoclusters and Water with the Effective Fragment Potential Method. ACS Omega, 5(13), 7446–7455. https://doi.org/10.1021/acsomega.0c00132

Wang, Y., Liu, P., Li, H., Li, T., Wang, P., Dong, J., Zhang, F., Chen, Z.-N., & Li, H. (2025). Heterogeneously Catalytic Synthesis of Au 13 Nanocluster . CCS Chemistry, 1–8. https://doi.org/10.31635/ccschem.025.202405142

Wang, Y., & Zhou, G. (2022). DFT Investigations of Aun Nano-Clusters Supported on TiO2 Nanotubes: Structures and Electronic Properties. Molecules, 27(9). https://doi.org/10.3390/molecules27092756

Westawker, L. P., Khusnutdinova, J. K., Wallick, R. F., & Mirica, L. M. (2023a). Palladium K-edge X-ray Absorption Spectroscopy Studies on Controlled Ligand Systems. Inorganic Chemistry, 62(51), 21128–21137. https://doi.org/10.1021/acs.inorgchem.3c03032

Westawker, L. P., Khusnutdinova, J. K., Wallick, R. F., & Mirica, L. M. (2023b). Palladium K-edge X-ray Absorption Spectroscopy Studies on Controlled Ligand Systems. Inorganic Chemistry, 62(51), 21128–21137. https://doi.org/10.1021/acs.inorgchem.3c03032

Zhu, B. C., Deng, P. J., Guo, J., & Kang, W. Bin. (2022). Computational Exploration on the Structural and Optical Properties of Gold-Doped Alkaline-Earth Magnesium AuMgn (n = 2–12) Nanoclusters: DFT Study. Frontiers in Chemistry, 10. https://doi.org/10.3389/fchem.2022.870985